Minimum sparkover voltage characteristics in air, sulphur-hexafluoride, and some solid dielectrics: A macroscopic approach

M. M. Kekez and P. Savic[a)]
Institute for Information Technology, National Research Council of Canada, Ottawa, Ontario K1A 0R6, Canada

(Received 7 November 1990; accepted for publication 22 February 1991)

Using a small number of plausible assumptions regarding the nature of the leader channel and the corona cloud in an electric discharge in a continuous medium, it is shown how a nonlinear first-order differential equation of the d'Alembert type can be derived which describes the history of the leader and corona cloud development in nondimensional terms. It is found that this solution can be used to derive a breakdown criterion which depends only on two material parameters, i.e., the minimum energy per unit length of the elongating leader channel and the average electric field in the corona cloud. These can be combined to form a single nondimensional parameter (Kekez number). The theory also shows how, for large gaps, the discharge must necessarily lead to the stepped-leader phenomenon. Comparison with experiments of other authors shows good agreement even for dielectrics of other than gaseous states of aggregation, where the concept of corona cloud requires some reinterpretation.

I. INTRODUCTION

It is generally realized that the physics of electrical breakdown in continuous media involves very complex mechanisms comprising many microscopic transitions and phenomena and requiring vast computational programs. Yet, breakdown in nearly all insulators and states of aggregation displays a surprising number of common macroscopic features. We propose in the following to use these features, together with the "lumped parameter" approach to derive useful criteria for minimum sparkover voltage.

We intend to show that the use of an approximate method, involving the Laplace field description of the electric field inside the gap, offers an opportunity to get an overall macroscopic picture of the discharge behavior.

This paper is aimed toward understanding the temporal evolution of the leader discharge observed in streak records. For clarity, we shall restrict ourself to the case of the so-called continuous leader development, although the method is sufficiently flexible to apply to stepped-leader phenomena. The goal of the paper is to broaden the theoretical base in determining the self-similar properties of minimum sparkover voltage in air for both polarity in rod-plane (0.1–30-m) gaps[1] as well as in other dielectrics and to incorporate the experimental evidence relating to the leader velocity extended over a wide range of current and spacing distances (0.09–2000 A and 0.01–1750 m, respectively) with the hypersonic detonation and hypersonic flame models proposed.[2]

The data collected by Cooke and Cookson[3] for a wide range of gas densities extending to the liquid phase in small semiuniform gap seem to suggest that the density of the matter alone determines the insulation strength. They claim that it is immaterial whether the matter is in gaseous, liquid, and/or solid-state form. This is perhaps too sweeping an assertion, but the quantity of matter as expressed in the density, not quality, determines the breakdown field strength to a first approximation according to the data presented.

The present paper may be viewed as an attempt to reconcile the findings of Cooke and Cookson with other well-established experimental results, such as those relating to current through the discharge, leader speed, and voltage wave form. We propose to show this by means of a simple macroscopic theory. For a beautiful example of the experimental studies upon which we base our work, see the paper by Chalmers *et al.*[4] on discharges in short point-plane gaps in SF_6.

II. FORMULATION OF THE PROBLEM

In analogy to the breakdown between parallel plates where the breakdown voltage V_s is proportional to the product of distance d and the gap density N (pressure P), i.e., Paschen's law ($V_s/pd = E/p = \text{const}$), we shall take conditions to be the same as in a rod-plane geometry. Since this configuration is a highly inhomogeneous one, the average field inside the corona (streamer) cloud is taken to be constant for a given dielectric density. By definition,

$$\bar{E} = \frac{V - V_c}{r_c}, \tag{1}$$

where the quantities are specified in Fig. 1. Spherical symmetry of the corona is assumed to hold over the whole motion.

This may be understood in terms of an interplay between the processes of ionization and de-ionization. If locally the ionization field is exceeded, the creation of new particles tends to shield the field and further ionization is inhibited; on the other hand, if the local field falls substan-

[a)]Researcher Emeritus.

 0021-8979/91/117510-10$03.00

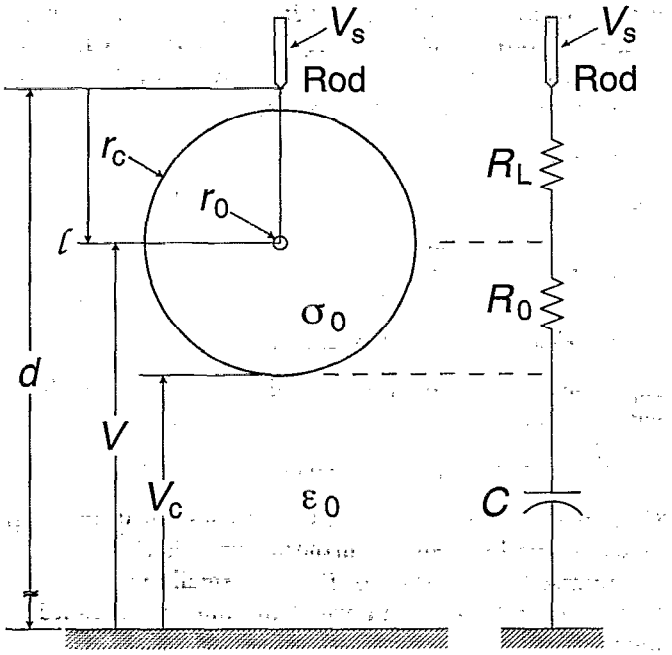

FIG. 1. A schematic diagram of the gas discharge structure (left) and of the equivalent circuit (right).

tially below this value, de-ionization sets in, and the local-field strength is thereby increased.

In zero-order approximation, the corona cloud can be considered to be a region of quasiuniform plasma, through which the current transport is assumed to be purely conductive (of conductivity σ_0). If we take the electrical contact between the leader tip and the corona cloud to be confined to the tip of radius r_0, the Laplacian field formulation demands that the effective resistance inside the cloud is

$$R_0=\left(\frac{1}{r_0}-\frac{1}{r_c}\right)\Big/(4\pi\sigma_0), \tag{2a}$$

for $r_c \gg r_0$,

$$R_0=(4\pi r_0\,\sigma_0)^{-1}, \tag{2b}$$

and equal to that between two concentric spheres. A Townsend generation-recombination mechanism takes place inside the corona cloud, while outside the fields are low; the dielectric has a tendency to attach free electrons; the degree of ionization is small; and for large gaps the displacement current effects, through the space capacity $C=4\pi\epsilon_0 r_c$ (it is assumed that the corona cloud is far from the electrodes), provide a current path between the corona cloud domain and the opposite electrode.

For the leader tip carrying to large degree the potential of the electrode from which it originates, the Laplacian formulation suggests that the field intensity at the tip is very large indeed. This causes not only electron multiplication via the Townsend coefficient, but also strong heating of electrons. The energy is deposited in the vicinity of the tip, and this energy supplied to the leader channel is transferred to it from the electrons and ions, enabling the channel to elongate. The processes is "tip specific"; i.e., most of the physical mechanism must be confined to a region close to the tip; the field is serving merely as a means of leading the current in and out of the tip zone. Two different mechanisms are possible. In the first, ionization causes the temperature of the gas to rise because of increased concentration of electric current. This temperature rise is again transmitted into the environment by either conduction or a shock wave, where it engenders further ionization. In the second mechanism, the new electrons generated by ionization diffuse ahead of the front, thereby advancing the region of maximum electric field which causes ionization at this new location.

Exactly analogous are the conditions in the electrically supported combustion and detonation process.[5] This can be extended to encompass mathematically similar mechanisms of creep and solid fractures.[6] On the basis of these observations, we propose to show in the following that the minimum sparkover voltage can be expressed in terms of the minimum average field inside the corona cloud, $\bar{E}$, required to sustain the electrically supported detonation or combustion (flame) in the leader channel and by the minimum energy per unit length W that the channel receives. Below this minimum the flame (or detonation) is assumed to quench itself. W is defined as

$$W=VI/v, \tag{3a}$$

where v is the leader velocity; I and V are the current and the voltage at the tip, respectively.

Equation (3a) is based on the supposition that the total ionization per unit length of leader in the corona cloud is very low compared with that in the leader stem indicated in Fig. 1 by the letter l. In addition, we assume that most of the power supplied to the gap goes into the ionization process in the leader tip by being transferred from the term $R_0 I^2$ to the leader tip via the detonation and/or flame diffusion mechanism. Also, it is considered that no power is lost in the capacitive displacement process beyond the clouds and that the temperature of the leader plasma, kT, is less than the ionization potential V_i.

Hence, the ionization energy of a cylindrical piece of leader of radius r_0 and length l is $r_0^2\, l\pi n_e V_i$, where n_e is the electron density and W is given by

$$W=\pi l r_0^2 n_e V_i, \tag{3b}$$

and therefore an invariant of the process, provided r_0 is a fixed multiple of the Debye length, which was assumed to be the case.[7] Equation (3a) is of course a crude approximation; in the two-dimensional extension of the flame diffusion and the detonation model,[5] it was demonstrated that for continuous motion, the quantity W is proportional to the leader velocity in both diffusion and detonation. The minimum value for the energy per unit length corresponds to the minimum leader speed value. Although W can vary to some degree during a discharge, we are assuming as stated by Eqs. (3a) and (3b) that its mean value is constant as far as the minimum sparkover voltage characteristics are of concern.

It is clear that in our formulation the breakdown is a completely local event, unaffected by past or future condition.

The energy loss in a long leader stem plays an important role. Well downstream from the tip, the rapid expansions and overexpansions and subsequent recompression of the hot dense plasma of the leader tip leads to a condition where any shock decays into a sound wave. Since there the pressure inside the channel is almost equal to the outside, the channel itself can be considered a vertical unconfined arc.[8]

In our view the arc characteristics are not simply added to the sparkover voltage calculations, but are incorporated in the entire model through the governing differential equation. We suggest that the ratio of R_L/R_0 is the dominant factor where R_L is the total resistance of the leader channel:

$$R_L=(V_s-V)/I, \tag{4a}$$

where

$$I=\frac{\partial}{\partial t}(CV_c), \tag{4b}$$

and R_0 is given by Eq. (2a). We shall demonstrate that the channel will bridge the gap as long as $R_L/R_0 \ll 1$. If the channel is cooled down because of radiation-dominated losses, R_L will rise, the voltage at the tip V will fall (see Fig. 1), and the corona cloud radius r_c of Eq. (1) will shrink, causing R_0 to fall [Eq. (2a)]. The net result is the generation of short current pulses (as computed in the large-signal analysis[9]). This process, known also as the reillumination, will in turn reenergize the arc channel plasma, lowering the arc electric field and the overall value of the channel resistance R_L. In our model, the spacing between the current pulses is governed by the rate of the energy loss of the arc channel plasma following reillumination. From the pulsed power point of view, the breakdown is analogous to the application of a hammer (impact) force to a solid, i.e., exploitation of yield and threshold phenomena as in solid fracture.

III. ANALYSIS

According to the equivalent circuit (Fig. 1), we have three independent definitions of the total current I, namely, Eqs. (4a) and (4b) and the additional equation

$$I=(V-V_c)/R_0=\frac{\partial}{\partial t}(CV_c). \tag{4c}$$

From the four relations

$$\overline{E}=(V-V_c)/r_c, \quad V_s-V_c=I(R_L+R_0),$$

$$y=r_cV_c, \quad y'=\frac{dy}{dt},$$

we obtain the equation

$$V_s-y\overline{E}/(IR_0)=I(R_L+R_0),$$

which, together with the Eqs. (2b) and (4c) yield a nonlinear first-order differential equation of the d'Alembert type. Two important cases can be distinguished, namely, (a) if R_L is small ($V_s=V$), we obtain

$$y'^2-by'+cy=0, \tag{5}$$

where

$$y=r_cV_c, \quad y'=\frac{\partial y}{\partial t},$$

$$b=Vr_0\sigma_0/\epsilon_0, \quad c=(r_0\sigma_0/\epsilon_0)^2\overline{E}_0.$$

Equation (5) was obtained by multiplying V_c of Eq. (4b) with Eq. (4c):

$$\overline{E}r_c/(IR_0)=(r_0\sigma_0\overline{E}r_c)/(y'\epsilon_0)=1.$$

Here, both V_s and r_0 are considered constant in time, an assumption which will be further justified later.

In case (b), the value of R_L is not small in comparison with other resistance parameters and must be included as follows:

$$[1+(R_L/R_0)]\,y'^2-b_1y'+cy=0, \tag{6a}$$

and

$$b_1=V_sr_0\sigma_0/\epsilon_0. \tag{6b}$$

Examining our previous theoretical models (detonation and diffusion; see Kekez and Savic[5]), as well as the experimental evidence relating to leader speed v versus leader current I over a wide range of current and spacing distances[2] (0.09–2000 A and 0.01–175 m, respectively), we find, for continuous leader elongation and for the early stages of the final jump,

$$v\sim I^{2/3}. \tag{7a}$$

However, for later stages of the final jump and for the case of reillumination, it is advisable to take

$$v\sim I^2. \tag{7b}$$

In addition, for restricted range of elongation, it may be advisable to take

$$v=kI. \tag{7c}$$

Combining any of Eqs. (7a)–(7c) with the previous derivation, we find that the general form of the d'Alembert equation is preserved, albeit with changed parameters. First, we note that

$$I=4\pi\epsilon_0y',$$

and with Eq. (3), we have

$$\frac{R_L}{R_0}=\frac{V_sr_0\sigma_0}{\epsilon_0y'}-\frac{vWr_0\sigma_0}{4\pi\epsilon_0^2y'^2}, \tag{8}$$

which, when inserted in (6a), yields

$$y'^2-\frac{vWr_0\sigma_0}{4\pi\epsilon_0^2}+cy=0. \tag{9}$$

In the case where $W=$const and the leader velocity is proportional to current [Eq. (7c)], Eq. (9) becomes

$$y'^2 - b_2 y' + cy = 0,$$

where

$$b_2 = kWr_0\sigma_0/\epsilon_0. \tag{10}$$

Equation (9) can be rendered into the standard form of d'Alembert's equation by change of variables, leading to

$$Y'^2 - 2Y' + Y = 0,$$

the solution of which is

$$\tfrac{1}{2}(x - x_0) = \mp u + \ln(1 \pm u), \tag{11}$$

where

$$u = (1 - Y)^{1/2},$$

and x_0 is a time scale constant (i.e., integration constant). In terms of physical parameters, the new variables have the following values:

$$x = t\bar{E}/(2\pi\epsilon_0 R_0 V), \quad I = V(1 \pm u)/(2R_0), \tag{12}$$

$$2r_c\bar{E}/V = 1 \pm u, \quad 2V_c/V = 1 \mp u. \tag{13}$$

This procedure can be further generalized to include the case where the medium ahead of the corona cloud is preionized and possesses a conductivity σ_c. Thus, the space capacity C is shunted by a resistance and the solution of d'Alembert's equation becomes

$$\frac{1}{2}(x - x_0) = \frac{1}{1 - 2\alpha}\left(\ln(1 \pm u) - \frac{1 - \alpha}{\alpha}\ln[(1 + \alpha) \times (1 \pm \alpha u - \alpha)]\right), \tag{14}$$

where

$$\alpha = \frac{\sigma_c V}{2r_0\bar{E}\sigma_0},$$

and x, I, r_c, and V_c are as in Eqs. (12) and (13).

IV. RESULTS

r_c plots of Eqs. (13) and (14) are presented in Fig. 2. The current I, the corona cloud radius, and the voltages r_c and V_c, respectively, have two branches (Nos. 1 and 2), which are quite independent of each other.

Both branches start at $u = 1$ and end at $u = 0$, meeting each other at midpoint of the plot for a small value of α (from 10^{-6} to 0.01). In general, the major portion of branch No. 1 depicts the continuous mode of leader development: the gradual increase in the corona cloud radius r_c and in the current value $I = V(1 - u)/(2R_0)$, as well as the gradual decrease in the voltage between the corona cloud and plate, V_c. Branch No. 2 denotes shrinking of the corona cloud radius and the consequent decrease in the current value. In zero order this branch (No. 2) can be used to describe the breakdown, when the discharge is arrested, and/or the phase just prior the reillumination phase. However, on closer examination, the latter phase is better described if the d'Alembert equation is solved with the aid of Eq. (7b) where $v \sim I^2$, because there $r_c\bar{E}/V$

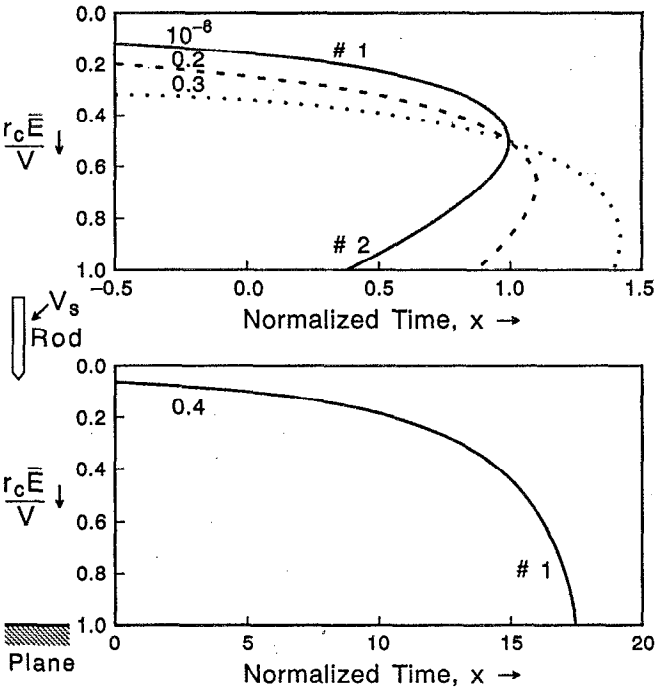

FIG. 2. Normalized corona cloud radius (in respect to the leader tip) vs normalized time Top: degree of preionization ahead of the corona cloud for α small to moderately high. Bottom: is high (= 0.4).

varies from 0 to 1 and the corona growing branch can be joined with the corona shrinking branch at any point inside the gap.

Figure 2 also shows that branch No. 1 occupies a larger portion of the plot as α rises. For $\alpha = 0.4$, branch No. 2 virtually disappears (see Fig. 2, bottom). To compare the analysis with experimental evidence, the position of the tip is determined by

$$l = \int_0^t v\,dt = \int_1^u v\frac{\partial t}{\partial x}\frac{\partial x}{\partial u}\,du. \tag{15a}$$

Here, $\partial x/\partial u$ and $\partial t/\partial x$ are calculated from Eqs. (11) and (12), respectively. With Eqs. (7c) and (12), the above integral is

$$l = \frac{-2\pi\epsilon_0 k}{\bar{E}}\int_1^u V^2 u\,du. \tag{15b}$$

Combining Eqs. (8) and (12), V of Eq. (15a) is

$$V = V_s/s, \tag{16}$$

with

$$s = 1 + m(1 - u), \quad m = R_l/(2R_0).$$

This makes possible to integrate Eq. (15) for branch No. 1. However, it is convenient to normalize both r_c and l with respect to the ratio $V_s/\bar{E}$. Hence,

$$L = \text{total length}/(V_s/\bar{E}) = r_c/(V_s/\bar{E}) + l/(V_s/\bar{E}), \tag{17}$$

and by integrating Eq. (15), we get

$$L = (1 - u)/(2s) + D[(m + 1)(s - 1)/s - \ln s]/m^2,$$

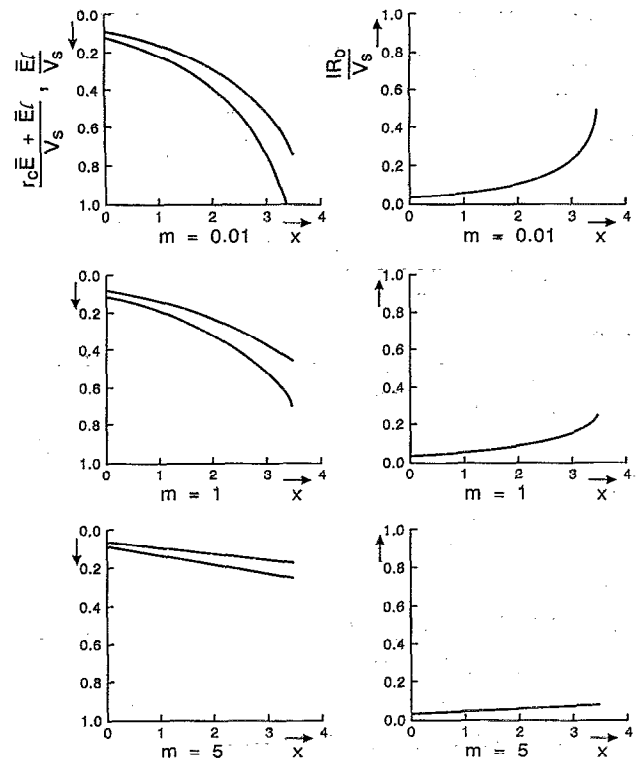

FIG. 3. The computed streak records (left) and the current wave forms (right) for three different values of the parameter $m = R_L/2R_0$. Upper trace depicts the leader head, while the lower one depicts the corona cloud edge. Here, $D=1.5$.

where

$$D=2\pi\epsilon_0 k V_s. \tag{18}$$

The terms in Eq. (18) result from the first and second terms of Eq. (17), respectively. The plots of Eq. (18) are given in Fig. 3 for three different values of the parameter, m, together with the normalized current wave form:

$$IR_0/V_s=(1-u)/(2s). \tag{19}$$

There is no change in the wave forms when m varies from 10^{-4} to 10^{-1}. For $m>1$, the discharge is arrested. To get the discharge to bridge the gap (assumed to be given by the condition $L=1$), it is necessary either to increase V_s implicit in the constant D [Eq. (18)] or to decrease the value of R_L used in m.

If the relationship $v \sim I^{2/3}$ is adopted instead of $v \sim I$, we obtain similar plots. The computed streak records are nearly identical, although the analysis is very laborious. The major difference to the $v \sim I^{2/3}$ law is that in this case the parameter D contains the value of $R_0^{1/3}$. See Appendix A.

In general, R_0 given by Eq. (3) is determined in essence by the Townsend ionization-recombination and continuity equations and, as such, it is "gas specific." The law $v \sim I^{2/3}$ recognizes that there are differences in the computed streak records between the different gases; however, the law $v \sim I$ is "blind" to these observations. The current wave forms are rather insensitive to the value of m for early time of x (see Fig. 3) in both cases.

The method herewith proposed offers an opportunity to calculate the corona cloud-leader tip motion in the stepped leader phenomena by combining the d'Alembert solution of the $v \sim I^{2/3}$ law for the growing cloud with the $v \sim I^2$ for the shrinking cloud by applying the simple Townsend charge with the current continuity equations to evaluate the changes in the value of R_0. Part of this task was already demonstrated in the work by Kekez, Savic, and Lougheed.[9] There, a simple theory for Trichel discharges in gases was proposed, in which the corona region was assumed to be describable in terms of a Townsend generation-recombination mechanism, while the other drift region was deemed subject to photoionization-attachment processes, together with displacement current effects. The resulting pair of first-order nonlinear differential equations was examined and found to readily yield the development of current pulse shapes, stability limits, frequency, and damping coefficient.

The remaining task in the current analysis (to be published) will involve inclusion of the characteristics of the leader channel. These can be approximated by the experimental volt-ampere data of long free vertical arcs (for air, see the work by Latham[8]). The loss of energy due to radiation and conduction in vertical arcs causes increase in leader channel resistance and, in turn, slowing down of the leader propagation rate (m rises in Fig. 3). As a result of this process, the corona cloud radius starts shrinking in respect to the leader tip, causing a fall in the R_0 value and a rise in I. Note that the differential equation is highly nonlinear; hence, a large, sharp current pulse would follow and the leader channel will be reenergized, causing m to fall and the channel to elongate; the process is then repeated until the gap is bridged. This method should yield a relationship between the average current and pulse frequency during stepped-leader phenomena, as well as the time separation between the current pulses. Furthermore, this will relate these phenomena to those of a Trichel-type gas discharge behavior, even though the parameters involved there are of different order of magnitude when compared with Trichel discharges.

Let us now evaluate the average value of the current for the case when $m = R_L/2R_0$ is small, i.e., for the condition of continuous leader elongation. In general, using equivalent circuits there are two distinct possibilities relating to the individual branches (Nos. 1 and 2) presented in Fig. 2. The analysis is simplified when u is close to 1. For branch No. 2, it was demonstrated[1] that the overall potential distribution from the leader tip to the plane resembles that of the initial phase of charging the capacitor C via the resistors R_0 and R_L. This gives

$$\frac{\partial V_c}{\partial t}=-\frac{\partial V}{\partial t},$$

and

$$\frac{\partial R_L}{\partial t}=(1+2R_L/R_0)/C.$$

TABLE I. $\overline{f(u)}$ function.

u	0	0.1	0.2
$\overline{f(u)}$	$\frac{11}{12}$	1.01	1.11

On the other hand, the overall condition for branch No. 1 can be obtained directly with aid of Fig. 1:

$$V_c + I(R_0 + R_L) = V_s, \quad V = V_s - R_L I,$$

the differential of which is

$$\frac{\partial V_c}{\partial t} = -\frac{\partial}{\partial t}[I(R_0 + R_L)], \quad \frac{\partial V}{\partial t} = -\frac{\partial}{\partial t}(IR_L), \tag{20}$$

and for u close to 1, I can be considered to be nearly constant, making

$$\frac{\partial V_c}{\partial t} = \frac{\partial V}{\partial t}. \tag{21}$$

Since by definition

$$I = 4\pi\epsilon_0 y' = 4\pi\epsilon_0 \left(\frac{\partial}{\partial t} r_c V_c\right), \tag{22}$$

and for the growing branch (No. 1),

$$r_c = (1-u)V/(2\overline{E}), \quad V_c = (1+u)V/2, \tag{23}$$

we have

$$\frac{\partial r_c}{\partial t} = \frac{1-u}{2\overline{E}} \frac{\partial V}{\partial t} - \frac{I}{4\pi\epsilon_0 u V}. \tag{24}$$

By combining Eq. (22) with (23) and (24), we have

$$I = -4\pi\epsilon_0 \frac{V}{\overline{E}} \frac{\partial V}{\partial t}\left[\frac{u(1+u)}{2} + u\left(\frac{\partial V_c}{\partial t}\right)\Big/\left(\frac{\partial V}{\partial t}\right)\right]. \tag{25}$$

With Eq. (21), the terms in the brackets are equal to

$$f(u) = (3+u)u/2,$$

the average value of which is

$$\overline{f(u)} = \frac{1}{u-1}\int_1^u f(u)\,du,$$

and its numerical values are given in Table I. The remaining problem concerns the derivation of a realistic breakdown criterion. Observations show that breakdown occurs irreversibly and nonarrestably when the farther edge of the corona cloud touches the electrode opposite the one from which the leader originates and when the voltage at the rod maintains its original value $(\partial V_s/\partial t) = 0$. In a mathematical presentation of the model, this implies that for the cloud reaching the opposite place, $u \to 0$.

$\overline{f(u)}$ permits us to simplify Eq. (25) as

$$I = -4\pi\epsilon_0 \frac{V}{\overline{E}} \frac{dV}{dt} = -4\pi\epsilon_0 \frac{V}{\overline{E}} v \frac{dV}{dl}. \tag{26}$$

For positive V, I is positive because dV/dl is negative. Multiplying (26) by V and integrating it for the leader tip motion from $l=0$, where $V = V_s$, to $l = d - r_c$, where $V_c = 0$, we set

$$\frac{4\pi\epsilon_0}{\overline{E}} \int_{V(d-r_c)}^{V_s} V^2\,dV = -\int_{d-r_c}^{0} \frac{VI}{v}\,dl,$$

whereby the above expression is of identical form as the one derived earlier[1] with the following results obtained on integration under the condition $V_s \gg V(d - r_c)$:

$$V_s^3 + pV_s \mp q = 0. \tag{27}$$

The only real root of this is

$$V_s = \pm(4p/3)^{1/2} \sinh\theta, \tag{28a}$$

where

$$\sinh 3\theta = (27q^2/4p^3)^{1/2}.$$

Here,

$$p = 3W/(4\pi\epsilon_0), \quad q = 3\overline{E}Wd/(4\pi\epsilon_0), \text{ and } W = VI/v.$$

Equation (28) has the following two asymptotic limits:

$$V_s = \overline{E}d,$$

and

$$V_s = [3\overline{E}Wd/(4\pi\epsilon_0)]^{1/3}. \tag{28c}$$

A simplified version of Eq. (27) is given in Appendix B.

V. COMPARISON WITH EXPERIMENTAL DATA

We shall now examine Eq. (28) in the light of experimental evidence for a rod-plane gap with either polarity. We concentrate our attention on the data for SF_6; results for air discussed elsewhere[1] are reproduced here for easy comparison. Results obtained under ac conditions in Mylar, P.E., and PMMA are also included for the sake of further discussion. Our findings are given in Fig. 4. The computed curves are the solid lines evaluated with the aid of the parameter given in Table II and presented in Table III. Broken lines are the extrapolation of the solid curves where the experimental evidence is not available at present.

In the case of SF_6, much experimental effort has been expended to investigate the sparkover characteristics in rod-plane configuration in an attempt to answer the apparent inconsistencies arising from the details of field divergence at the rod, gap irradiation, impulse wave shape, and duration as a function of the gas density (pressure) and/or the gap separation. By contrast with air, where it has been possible to reproduce the breakdown data with fairly reliable methods, SF_6 became of technological interest in comparatively short gaps of less than 50 cm because of the semisaturation feature of the breakdown voltage at larger gaps (see Fig. 3). Many investigators use the gas density (pressure) as a variable (sometimes increased to tens of atmospheres) to further optimize the use of SF_6 as a gaseous insulant in metal-clad equipment. Here, it becomes apparent that SF_6 characteristics become susceptible to high-field sites caused by either roughness of the stressed

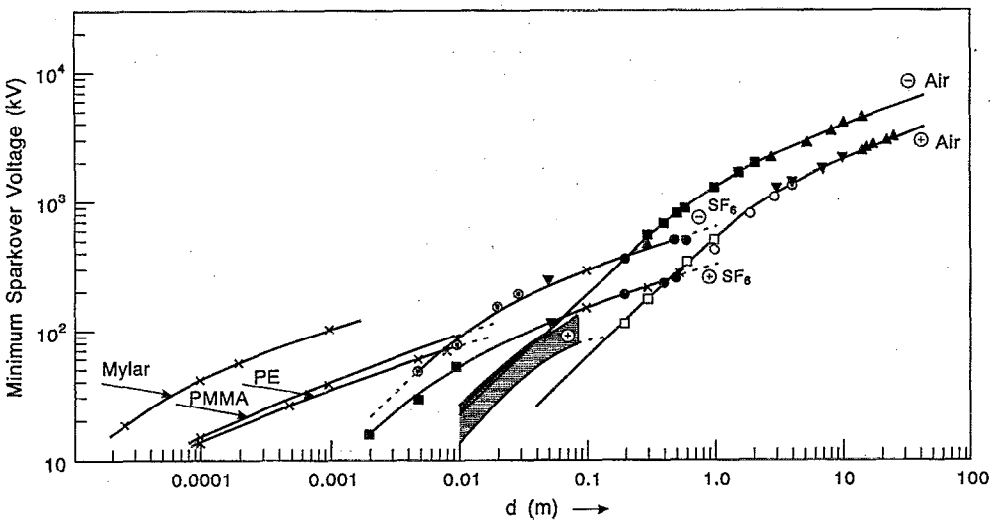

FIG. 4. The minimum sparkover voltage (absolute value, V_s against gap length, d for rod-plane gaps). Theory: solid lines. Experimental points for SF_6: (■) Farish, Ibrahim, and Korasli (Ref. 10), (×) Takuma, (Ref. 11) (●) Pigini, Rizzi, and Brambilla (Ref. 12), (●) Aris and Strivastava (Ref. 13), (▲) Kurimoto, Aked, and Tedford (Ref. 14) and (⊙) Kuffel and Yializis (Ref. 15). For air, see Kekez (Ref. 1). For Mylar, PMMA, and P. E., see Cuddihy (Ref. 16).

surfaces or unwanted presence of dust-particle contamination. In addition, SF_6 displays an anomalous behavior in the breakdown characteristics as a function of density (pressure) for a given gap. For example, at lower pressure (below 2 bars), the breakdown curve exhibits the familiar steep increase in breakdown voltage with pressure, generally described as "corona-stabilized breakdown," followed by a fall in breakdown voltage at moderate pressure until at high pressure it coincides with the corona inception voltage curve. This anomalous feature in SF_6 is similar to that found for rod-plane gaps in air and depicted by the shaded area (designated by the symbol + and − for a positive and negative rod-plane gap, respectively).

In view of the above-mentioned complexity of SF_6 behavior, comparison will be made between the formulas (and/or experimental values) of other authors, suitably normalized to remove local experimental parameters, and our expression (Table III). In that formula, values of $W=VI/v$ were found from the work of Niemeyer and Pinnekamp,[17] as their leader channel propagates smoothly along insulator surfaces.

Smooth leader elongation is required by expression (28). Most of the experimental data show that the leader extends with intermitted reillumination steps. From the data by Niemeyer and Pinnekamp, $I=0.34$ A, $V=35$ kV, and $v=10^5$ m/s, we get $W=0.12$ J/m for positive polarity in SF_6. Similarly, for negative polarity we get $W=0.81$ J/m, for which the average field in the corona (streamer) cloud is taken to be 87 kV/cm at 1 atm following closely the suggestion by Mesetti *et al.*[18] It turns out that this value is equal to the maximum value of the uniform field strength as determined by Berril, Christensen, and Pedersen[19] using the Paschen curve to evaluate the lowering of the breakdown voltage caused by surface defects. The measured (or estimated) average values of the field in the corona cloud under positive polarity vary considerably in the literature from as low as 30 kV/cm to as high as 70 kV/cm at 1 atm of SF_6. The value of 62 kV/cm was adopted here to match Eq. (28) and the experimental results given in Fig. 4. No attempt was made to do any "fine tuning" in choosing $\overline{E}$ and W to get the overall best comparison (see Table III) over the whole range of gap length between the present expression and the experimental data of other authors. It appears, therefore, that the two material parameters W and $\overline{E}$, when estimated from one set of experimental results and incorporated in our expression (28), are well suited to represent large numbers of experimental results of other authors over a wide range of physical conditions. In addition, in spite of the relative crudity of the theory, the qualitative course of the curves in Fig. 3 is in general agreement with experimental findings.

TABLE II. Sparkover voltage parameters.

	$\overline{E}_{+\,(dc)}$ (kV/cm)	$\overline{E}_{-\,(dc)}$ (kV/cm)	W_+ (J/m)	W_- (J/m)
Dielectrics	$E_{(ac)}$ (kV/cm)		$W_{(ac)}$ (J/m)	
air	5	16	80	118
SF_6	62	87	0.12	0.81
Mylar	8252		0.030	
P.E.	2800		0.002 83	
PMMA	3166		0.003 65	

We shall now focus our attention on solid insulators. In the work by Cuddihy,[16] the concept of "intrinsic" dielectric strength of this type of insulation material is proposed. Breakdown occurs at a constant value of the intrinsic field strength E for each material determined when the thickness of solid insulation curve is extrapolated to zero and when the leader channel termed "electrical tree" has a needlelike asperity of a constant value at the tip of the radius of curvature equal to 30.5 μm. This radius is independent of actual electrode geometry. The author's mathematical derivation can be interpreted as an approximation of Eq. (28) by assuming that his values of intrinsic field strength can be equated with our value of the average field in the corona cloud and by assuming that his radius of curvature can be expressed in terms of our parameter W. His value of the intrinsic field are reproduced in Table III for low-density polyethylene (P.E.), polymethyl methacry-

TABLE III. Sparkover voltage in rod-plane gap d.

References	Conditions	Formula for V_s (kV vs gap d)	Range of d (m) (tentative)	Comparison	for gap d		
					percent		
Farish and co-workers (Ref. 10)	SF_6, positive		2–10 (mm)	d (mm)	2	5	10
				%	−1.98	−12.4	−0.33
Pigini and co-workers (Ref. 12)	dc, 1 atm	$65\ d^{0.3}$ (cm)	0.05–0.5 (m)	d (cm)	10	30	50
				%	0.85	−2.54	−7.46
Present work		70.99 sinh θ sinh $3\theta = 152.80d$ (m)	0.002–0.5 (m)				
Kuffel and Yializis (Ref. 15)	SF_6, negative			d (mm)	5	20	50
				%	2.9	9.58	0.58
Pigini and co-workers (Ref. 12)	dc, 1 atm	$136.5\ d^{0.3}$ (cm)	0.05–0.5 (m)	d (cm)	10	30	50
				%	13	3.42	0.32
Present work		170.763 sinh θ sinh $3\theta = 152.89d$ (m)	0.002–0.5 (m)				
Cuddihy (Ref. 16)	Mylar, ac	$82.5226\ \frac{d\ (\text{mm})}{[d\ (\text{mm}) + 0.0305]^{2/3}}$	0.025–1 (mm)	d (mm)	0.025	0.1	1
				%	−4.06	−5.57	−4.75
Present work		32.863 sinh θ sinh $3\theta = 75.33d$ (mm)					
Cuddihy (Ref. 16)	P.E., ac	$28.2\ \frac{d\ (\text{mm})}{[d\ (\text{mm}) + 0.0305]^{0.67}}$	0.1–10 (mm)	d (mm)	0.1	0.5	8
				%	0.02	2.63	0.84
Present work		10 093.56 sinh θ sinh $3\theta = 83.227\ 33\ d$ (mm)					
Cuddihy (Ref. 16)	PMMA, ac	$31.16\ \frac{d\ (\text{mm})}{[d\ (\text{mm}) + 0.0221]^{0.63}}$	0.1–10 (mm)	d (mm)	0.1	1	8
				%	4.63	−5.52	6.99
Present work		11 462.98 sinh θ sinh $3\theta = 81.549d$ (mm)					

late (PMMA-acrylic), and Mylar. The value for W was determined here with the aid of Eq. (28c) and the experimental data summarized in the work by Cuddihy.

The order of magnitude of the energy needed to generate a volume of the corona cloud, $4\pi r_c^3/3$, can be obtained as suggested by Felici[20] by summing the terms corresponding to the various processes involved, i.e., vaporization of solid dielectric, decomposition, ionization, and displacement. Each term can be expressed in terms of $\epsilon_0\overline{E}^2/2$ of the electrostatic energy caused by the average value of the corona field $\overline{E}$. Assuming that for all three dielectrics $\epsilon_r/\epsilon_0 = 1$ and that the leader tip "mops up" the energy of the cloud completely, then the upper limit of the value of r_c can be estimated when the displacement of electrostatic energy is equated to the minimum energy per unit length W:

$$\frac{\partial}{\partial r_c}\left[\frac{4}{3}\pi r_c^3\left(\frac{\epsilon_0\overline{E}^2}{2}\right)\right] = W, \tag{29}$$

making

$$r_c = [W/(2\pi\epsilon_0)]^{1/2}/\overline{E}.$$

Using the value for E and W given in Table II, r_c is evaluated and the results are given in Table IV. We see that r_c for all three solid dielectrics has about the same value and falls in the same range as the radius of curvature of needlelike asperity of 30.5 μm suggested by the work of Cuddihy. This justifies the above assumption about the relation between W and r_c.

The same result can be obtained using the approach of Hora *et al.*,[7] who calculated the surface tension in a dense, laser-generated plasma. From that treatment, it emerges that in solids, the initial surface asperity and corona edge are separated by a distance of the order of the Debye length. This justifies the time independence of r_c in Eq. (29).

VI. CONCLUSIONS

Calculated values of the minimum sparkover voltage are in good agreement with the measured value of over 7 decades of gap width in a range from conditions of thin-(2.5-μm) film Mylar up to 35 m in air. It is believed that the present concept could be expanded to cover many other dielectrics providing that the quantity W becomes available. In this way the various dielectrics can be evaluated and the search for useful new dielectrics can be rationalized. It is hoped that properly chosen strata of dielectrics

TABLE IV. Theoretical value of r_c.

Mylar	28.10 μm
P.E.	25.40 μm
PMMA	25.57 μm

will exhibit synergism (i.e., the compounded stack may exhibit a dielectric strength in excess of that expected from the sum of properties of separate dielectrics). These, combined with current progress on high-temperature superconductors, may lead to an entirely new class of fast (minimum discharge time) high-energy density (J/cm^3), pulsed-power systems needed to promote further progress in the field of high-temperature (fusion) plasma generation as well as in the field of micromachining.

The present theoretical model utilizes the following simple and plausible assumptions: (a) Townsend generation-recombination mechanisms dominate in the corona cloud, making this a quasihomogeneous region. (b) The average value of E/p is constant in the cloud. (c) The known simple power function between leader speed and leader current has been applied. (d) The long leader stem is considered to have the properties of a conventional arc, as far as its electric-field-current characteristic is concerned. (e) The interaction between (a) and (d) is suggested to account for the stepped-leader phenomena in long gaps.

We have shown that the function of the corona cloud, in the mechanism of breakdown, is not merely to increase the effective length of the leader, but to provide a capacitive coupling across the nonconducting region between the corona edge and the far electrode. This also explains in part the presence of the familiar "U curve" of breakdown with rapidly varying gap voltage.

For continuous leader elongation, the breakdown is seen to be a function of a single nondimensional parameter s. See Appendix B. This quantity is proportional (though not equal) to the ratio of the energy density in the leader stem to the electrostatic energy density in the corona cloud, both material properties of the medium. This parameter, for which the name Kekez number has been proposed, is the inverse of the "electric Reynolds number" sometimes used in magnetohydrodynamics.[21]

Another type of breakdown occurs in stepped-leader phenomena (in long gaps). The core temperature in long channels depends on the current flow. Conduction and radiation determine the energy balance within the core and these quantities govern in turn the value of the resistance R_L in the stem. When R_L has a large value, the corona cloud will not reach the opposite electrode at large values of the nondimensional time x greater than that at which $u=0$. At this point, the propagation becomes self-arrested. Conditions are now right for the motion to enter branch No. 2 and the corona cloud to shrink, contributing to a gradual rise in current until the positive feedback, dictated by the differential equation, produces a large current impulse. The net result is an increase in the temperature of core channel plasma, and the cycle starts anew.

Further work is in progress to summarize the most significant experimental results obtained in recent years. Such comprehensive review will attempt to show the existence of such a universal relationship among the dielectrics as originally suggested in the work by Cooke and Cookson.[3]

ACKNOWLEDGMENTS

The authors are deeply indebted to Dr. M. M. C. Collins and S. A. Mayman for their interest in the project. Equation (A2) was derived by S. Sychaleun. Comments by Dr. A. S. Podgorski and help by Dr. R. J. Densley are much appreciated.

APPENDIX A: $v \sim I^{2/3}$ LAW

Equation (9) of the main text is

$$y'^2 - \frac{r_0\sigma_0 W}{4\pi\epsilon_0^2} v + (r_0\sigma_0/\epsilon_0)^2 \bar{E} y = 0,$$

with $v = kI^{2/3} = k(4\pi\epsilon_0 y')^{2/3}$, where $y' = dy/dt$. Equation (9) becomes

$$y'^2 - \frac{r_0\sigma_0}{4\pi\epsilon_0^2} k(4\pi\epsilon_0 y')^{2/3} + (r_0\sigma_0/\epsilon_0)^2 \bar{E} y = 0.$$

Letting $y = AY$ and $t = BX$, the expression above reads

$$-Y'^2 + Y'^{2/3} - Y = 0.$$

If

$$A = [R_0^{1/2}(kW)^{3/2}]/\bar{E},$$

$$B = R_0^{1/4}(kW)^{3/4}\epsilon_0/(r_0\sigma_0\bar{E}),$$

the solution is

$$X - X_0 = -2u - 2u^{-1/3}, \quad Y = -u^2 + u^{3/3}, \quad Y' = u.$$

Since

$$\bar{E} r_c r_0\sigma_0/\epsilon_0 = y' = (A/B)Y',$$

we get

$$I = (V/R_0)u^{4/3}, \tag{A1}$$

and/or

$$r_c\bar{E}/V = u^{4/3}.$$

With the circuit equation [Eq. (8) of the main text] and (A1), we get

$$V = V_s/(1 + mu^{4/3}), \quad m = R_L/R_0.$$

The leader length was determined as before:

$$l = \int_0^t v\, dt = \int_0^u kI^{2/3} \frac{\partial t}{\partial X}\frac{\partial X}{\partial u} du,$$

but here,

$$\frac{\partial t}{\partial X} = B, \quad \frac{\partial X}{\partial u} = -2(1 - u^{-4/3}/3),$$

and with the auxiliary variable

$$x = mu^{4/3},$$

the above integral is

$$l = D_1 \int_0^x \frac{x^{2/3}}{(1+x)^{5/3}} dx + D_2 \int_0^x \frac{dx}{x^{1/3}(1+x)^{5/3}},$$

the solution of which is

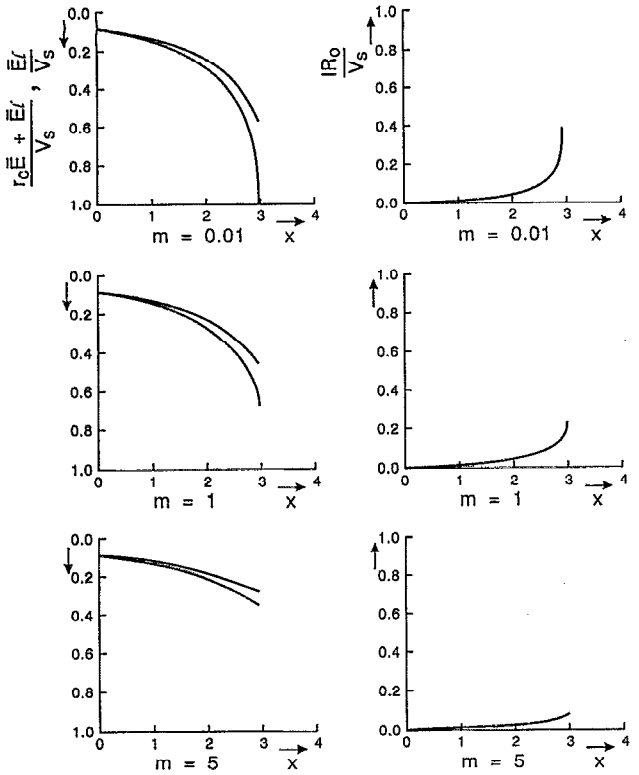

FIG. 5. As in Fig. 3, but for the $v \sim I^{2/3}$ law. Here, $D = 2$.

$$\frac{\bar{E}l}{V_s} = \frac{D}{m^2/3}\left[s^2 - \frac{2}{m}\left(-\frac{3}{2}s^2 - \ln(1-s) + \frac{1}{2}\ln(1+s+s^2) - 3^{1/2}\arctan\left(\frac{2s+1}{3^{1/2}}\right) + \frac{\pi}{2}\frac{1}{3^{1/2}}\right)\right],$$

where

$$s = [x/(1+x)]^{1/3}, \quad D = 3\pi\epsilon_0 k R_0^{1/3} V_s^{2/3}. \tag{A2}$$

Using Eqs. (A1) and (B1), the nondimensional distance of the corona cloud edge from the leader tip is

$$r_c\bar{E}/V_s = s^3/m,$$

and to the electrode is the sum of r_c and l. The results are given in Fig. 5.

APPENDIX B: SIMPLIFIED DERIVATION OF EQ. (27)

Equation (15b) of the main text is

$$l = -\frac{2\pi\epsilon_0 k}{\bar{E}}\int_1^u V^2 u\, du.$$

If $m \ll 1$, i.e., R_L is small, $V \simeq V_s$. The breakdown is defined as the point where the corona cloud edge reaches the ground. The leader length l is equal: $d - r_c$, where d = gap length; see Fig. 3, top. Hence, the above integral is

$$d - r_c = \pi\epsilon_0 k V_s^2/\bar{E}.$$

As $v = kI$, $W = VI/v$, and $V \simeq V_s$, we get

$$d - r_c = \pi\epsilon_0 V_s^3/(\bar{E}W). \tag{B1}$$

The value for r_c (at these conditions) corresponds to the branch No. 2 of Fig. 2 and given by Eq. (13) of the main text:

$$2r_c\bar{E}/V = 1 + u,$$

i.e., the cloud is shrinking; the process is very fast, as the "final jump" is launched followed by the return stroke. Thus, u maintains a value around 1. Hence,

$$r_c \simeq V_s/\bar{E}. \tag{B2}$$

Combining (B1) and (B2), we get

$$z^3 + sz - s = 0,$$

where z is equal to the nondimensional sparkover voltage $V_s/(\bar{E}d)$, and s is a single parameter $W/(\pi\epsilon_0\bar{E}^2d^2)$, which is the radio of the leader energy per unit length W to the electrostatic energy per unit length, $\pi\epsilon_0\bar{E}^2d^2$. In the main text, this single parameter s differs by a factor $\frac{4}{3}$; i.e., there, $s = W/(\frac{4}{3}\pi\epsilon_0\bar{E}^2d^2)$. This makes the present derivation for small d identical to Eq. (28b), whereas Eq. (28c) should read $V_s = \{[\bar{E}W/(\pi\epsilon_0)]d\}^{1/3}$ for very large d.

[1] M. M. Kekez, J. Phys. D **18**, 1813 (1985).
[2] M. M. Kekez, in *Proceedings of the 5th International Symposium Gaseous Dielectrics,* Knoxville, TN, 1987 (Pergamon, New York, 1987), pp. 104–117.
[3] C. M. Cooke and A. Cookson, IEEE Trans. Electr. Insul. **EI-13**, 239 (1978).
[4] I. D. Chalmers, I. Gallimerti, A. Gibert, and O. Farish, Proc. R. Soc. London A **412**, 285 (1987).
[5] M. M. Kekez and P. Savic, in Proceedings of the 9th International Conference Gas Discharges and Applications, Venice, Italy, 1988 (unpublished), pp. 415–419.
[6] R. Weichert and K. Schönert, J. Mech. Phys. Solids **22**, 172 (1974).
[7] H. Hora, S. Eliezer, M. P. Goldsworthy, R. J. Stening, and H. Szichman, in *Laser Interaction and Related Plasma Phenomena,* edited by H. Hora and G. H. Miley (Plenum, New York, 1988), Vol. 8, p. 293–325.
[8] D. J. Latham, Phys. Fluids **23**, 1710 (1980).
[9] M. M. Kekez, P. Savic, and G. Lougheed, J. Phys. D **15**, 1963 (1982).
[10] O. Farish, O. E. Ibrahim, and C. Koralsi, in Proceedings of the 5th International Conference Gas Discharges, Liverpool, 1978 (unpublished), pp. 320–323.
[11] R. Takuma, IEEE Trans. Electr. Insul. **EI-21**, 855 (1986).
[12] A. Pigini, G. Rizzi, and R. Brambilla, in Proceedings of the 7th International Conference Gas Discharge and Application, London, 1982 (unpublished), pp. 203–207.
[13] H. Aris and K. D. Srivastava, IEEE Trans. Power Apparat. Syst. **PAS-101**, 537 (1982).
[14] A. Kurimoto, A. Aked, and D. Tedford, in Proceedings of the 4th International Conference Gas Discharges, Swansea, UK, 1976 (unpublished), pp. 163–165.
[15] E. Kuffel and A. Yializis, IEEE Trans. Power Apparat. Syst. **PAS-97**, 2359 (1978).
[16] E. F. Cuddihy, IEEE Trans. Electr. Insul. **EI-22**, 573 (1987).
[17] L. Niemeyer and F. Pinnekamp, in Proceedings of the 3rd International Symposium Gaseous Dielectrics, Knoxville, TN, 1982 (unpublished), pp. 379–385.
[18] C. Masetti, A. Pigini, A. Bargigia, R. Brambilla, and B. Mazzoleni, in Proceedings of the 7th International Conference Gas Discharges and Applications, London, 1982 (unpublished), pp. 243–246.
[19] J. Berril, J. M. Christensen, and A. Pedersen, in Proceedings of the 7th International Conference Gas Discharges and Applications, London, 1982 (unpublished), pp. 266–268.
[20] N. J. Felici, IEEE Trans. Electr. Insul. **EI-23**, 497 (1988).
[21] N. S. Land, "A Compilation of Non-Dimensional Numbers," National Aeronautics and Space Administration Report No. NASA SP-274, 1972 (unpublished).